

On High and Extreme Wind Calibration Using ASCAT

Federica Polverari, Marcos Portabella, Wenming Lin, *Senior Member, IEEE*, Joseph W. Sapp, *Senior Member, IEEE*, Ad Stoffelen, *Senior Member, IEEE*, Zorana Jelenak, *Member, IEEE*, and Paul S. Chang, *Senior Member, IEEE*

Abstract—Accurate high and extreme sea surface wind observations are essential for meteorological, ocean, and climate applications. To properly assess and calibrate the current and future satellite-derived extreme winds, including those from the C-band scatterometers, building a consolidated high and extreme wind reference data set is crucial. In this work a new approach is presented to assess the consistency between moored buoys and Stepped-Frequency Microwave Radiometer (SFMR)-derived winds. To overcome the absence of abundant direct collocations between these two data sets, the reprocessed Advanced Scatterometer, (ASCAT)-A, winds at 12.5 km resolution, from 2009 to 2018, have been used to perform an indirect SFMR/buoy winds inter-comparison. The ASCAT/SFMR analysis reveals an ASCAT wind underestimation for winds above 15 m/s. SFMR measurements are calibrated using GPS drop-wind-sondes (dropsonde) data and averaged along-track to represent ASCAT spatially. On the other hand, ASCAT and buoy winds are in good agreement up to 25 m/s. The buoy high-wind quality has been confirmed using a triple collocation approach. In comparing these results, both SFMR and buoy winds appear to be highly correlated with ASCAT at the high wind regime, however, they show a very different wind speed scaling. An SFMR-based re-calibration of ASCAT winds is proposed, the so-called ASCAT dropsonde-scale winds, for use by the extreme wind operational community. However, further work is required to reconcile dropsonde (thus SFMR) and buoy wind measurements under extreme wind conditions.

Index Terms—High and extreme wind speeds, microwave radiometry, ocean wind reference, spaceborne scatterometry

I. INTRODUCTION

GLOBAL information on the motion near the ocean surface is generally lacking, limiting the physical modelling capabilities of the forcing of the world's water surfaces by the atmosphere [1]. This also limits our knowledge of the exchange

of momentum across the ocean-atmosphere interface, affecting meteorological and ocean applications [2]. A particularly pressing requirement in the Ocean Surface Vector Wind (OSVW) community is to obtain reliable extreme winds in hurricanes (> 30 m/s) from satellite wind scatterometers or radiometers, since extreme wind, storm surge and wave forecasts for societal warning are a high priority in nowcasting as well as in Numerical Weather Prediction (NWP).

Scatterometers provide 10-m stress-equivalent winds (U_{10S}) [3], with a grid resolution of 12.5 km or 25 km. They have proven to be very effective for wind vector retrieval [4]. Over the years, improvements have been done on the development of the empirical Geophysical Model Functions (GMFs) in order to obtain more accurate wind estimates with respect to in situ measurements [5]. However, developing and verifying wind scatterometer processing algorithms for high and extreme winds is challenging, since in situ wind measurements are scarce and they may be hazardous and unreliable. Moreover, theoretical statistical descriptions of the high-wind ocean surface, where patchy foam, droplets, spume and wave breaking occur are much simplified, while the microwave interaction on cm scales is rather complex.

The European Organization for the Exploitation of Meteorological Satellites (EUMETSAT)-funded “C-band High and Extreme-Force Speeds (CHEFS)” project aims at assessing the extreme wind capabilities of the next generation of C-band wind scatterometers on-board Metop Second Generation (SG) [6], in order to provide reliable extreme ocean surface vector wind information in open ocean and marine coastal regions, where generally limited in-situ measurement capability exists. To this end, an important goal within CHEFS is to provide an appropriate and consolidated high and extreme-wind reference data set at scatterometer scales, based on in-situ wind references. This reference is crucial for purposes of satellite

This work was supported by the Ministry of Science and Innovation, Spain, through the National R&D Plan under L-BAND project (ESP2017-89463-C3-1-R) and by EUMETSAT, through the Tender 16_166 - STC under CHEFS project (EUM/CO/16/4600001953).

F. Polverari was with the Institute of Marine Sciences, Barcelona, 08003 Spain. (e-mail: federica.polverari@jpl.nasa.gov).

M. Portabella is with the Institute of Marine Sciences, Barcelona, 08003 Spain (e-mail: portabella@icm.csic.es).

W. Lin is with Nanjing University of Information Science and Technology, Nanjing, China (e-mail: wenminglin@nuist.edu.cn).

J. W. Sapp is with Global Science & Technology (GST), Inc., Greenbelt, MD 20770, USA. He is also with NOAA/NESDIS Center for Satellite

Applications Research (STAR), College Park, MD 20740, USA (e-mail: joe.sapp@noaa.gov).

A. Stoffelen is with the Royal Netherlands Meteorological Institute (KNMI), De Bilt 3730 AE, The Netherlands (e-mail: ad.stoffelen@knmi.nl).

Z. Jelenak is with NOAA/NESDIS Center for Satellite Applications Research (STAR), College Park, MD 20740, USA. She is also with University Corporation for Atmospheric Research, Boulder, CO 80307, USA (e-mail: zorana.jelenak@noaa.gov).

P. S. Chang is with NOAA/NESDIS Center for Satellite Applications Research (STAR), College Park, MD 20740, USA (e-mail: paul.s.chang@noaa.gov).

ocean surface wind calibration and validation.

On the one hand, moored buoy data are generally used as absolute reference to calibrate the scatterometer wind GMFs, however, for very high and extreme winds above 25 m/s, moored buoys may not be reliable. Moreover, controversy exists in the OSVW satellite community on the quality of moored buoys above 15 m/s rather than 25 m/s [7]. On the other hand, the Ocean Surface Winds Team (OSWT) at the National Oceanic and Atmospheric Administration (NOAA)/National Environmental Satellite, Data, and Information Service (NESDIS)/Center for Satellite Applications and Research (STAR) (hereafter as NOAA/NESDIS/STAR OSWT) routinely fly into hurricanes and extratropical cyclones to collect measurements at high and extreme wind conditions. During each flight, the NOAA Aircraft Operations Center (AOC) operate the aircraft-based Stepped-Frequency Microwave Radiometer (SFMR), built by ProSensing, Inc. of Amherst, MA, USA [8]. SFMR is a passive nadir-looking instrument, that measures the brightness temperature (T_B) of the ocean surface at six different C-band frequencies. By using a retrieval algorithm, simultaneous retrievals of 10-m surface wind speed and rain rate are obtained [9, 10]. In addition, they also drop Global Positioning System (GPS) drop-wind-sondes (hereafter dropsondes), which measure wind speed, direction, pressure, temperature and relative humidity from the moment they are launched until they reach the ocean surface [11]. However, the dropsondes can fail in reporting the winds at the surface and, even when they do, the measured surface winds can be compromised by surface waves and wind gust effects. Therefore, the 10 m surface winds are usually estimated by layer-averaged winds [11, 12]. Such estimates are then used as reference to calibrate SFMR wind speeds. However, the dropsonde 10-m surface wind accuracy estimate is still an open issue within the ocean wind community and analysis of these layer-averaging methods are needed in order to better assess their impact on the SFMR winds.

In this scenario, both SFMR and buoy winds represent possible candidates to evaluate and possibly correct scatterometer winds in the high wind regime. However, direct SFMR and buoy collocations were not available to carry out a direct buoy/SFMR wind comparison to assess the consistency between these two data sets. Therefore, we present a new approach, which uses collocated wind data from the Advanced SCATterometer (ASCAT) onboard the EUMETSAT Metop-A satellite (hereafter as ASCAT-A) to bridge buoy and SFMR wind comparisons, i.e., on the one hand, we analyze SFMR and ASCAT-A collocations and, on the other, buoy and ASCAT-A collocations. Ten years of reprocessed and stable ASCAT-A surface winds from 2009 to 2018 are used [13, 14].

The present work is organized as follows: in Section 2 the collected data sets are discussed; Section 3 describes the methodology used to build the ASCAT/SFMR and the ASCAT/buoy wind collocations; Section 4 shows a comprehensive statistical analysis of both SFMR and buoy winds using ASCAT data as reference, in which a dropsonde-scale correction of ASCAT winds is proposed; finally, the conclusions can be found in Section 5.

II. DATA COLLECTION

A. SFMR Data

For this work, the NOAA/NESDIS/STAR OSWT provided ten years of reprocessed SFMR wind speed retrievals from 2009 to 2018. This data set has been acquired by the many NOAA WP-3D and U.S. Air Force Reserve Command (AFRC) flights over ten hurricane seasons.

The NOAA/NESDIS/STAR OSWT has reprocessed the SFMR dataset by using a new version of their GMF that corrects an approximate 10% low bias observed in the SFMR wind retrievals with respect to dropsondes, for winds ranging between 15 m/s and 45 m/s [10]. As mentioned in [10, 15], the validity of the SFMR low wind speeds (<15 m/s) and low rain rate (<10 mm/h) are questionable due to the sensitivity of the instrument to physical processes that need to be better understood.

Each year an in-flight ocean calibration is performed to adjust the T_B calibration equation for each channel to reflect the actual conditions [10]. The NOAA/NESDIS/STAR OSWT has inspected the provided wind data set to ensure that wind retrievals are good in terms of instrument calibration. In particular, they have excluded those winds whose corresponding T_B values were not considered as reliable, because of: (i) T_B differences amongst the six channels higher than 2K, suggesting the presence in the T_B calibration equation of possible errors that could not be corrected; (ii) the presence of a high amount of noise in the T_B channels.

The wind retrievals are provided at a frequency of 1 Hz. A quality control flag is available in the wind products in order to discriminate the valid wind solutions from those questionable or invalid. In this study, only the valid solutions are used. In terms of geolocation accuracy, most NOAA WP-3D flights have more accurate information than AFRC flights. This is due to the fact that AFRC geolocation (latitude/longitude) information is archived in floating numbers with a precision of only two decimals.

B. Re-processed ASCAT Wind Products with ERA5

The ASCAT-Level 2 ocean wind products are produced and publicly distributed by the EUMETSAT Ocean and Sea Ice Satellite Application Facility (OSI SAF) at the the Royal Netherlands Meteorological Institute (KNMI). Other agencies have also released their ASCAT-A wind products. Remote Sensing Systems (RSS) have fully reprocessed the ASCAT-A wind data in order to implement a new GMF developed at RSS [16]. With respect to their previous data release, major changes are seen at wind speeds above 30 m/s [17]. The NOAA/NESDIS/STAR OSWT has also processed the ASCAT-A wind data with a GMF that aims to improve the ASCAT-A wind retrieval at high wind regimes [18].

In this work, we have used the latest version of the reprocessed EUMETSAT OSI SAF ASCAT-A wind data products developed at KNMI [14]. This data set was reprocessed by using the European Centre for Medium-Range Weather Forecasts (ECMWF) Re-Analysis (ERA)-Interim model winds. However, ERA-Interim has the coarsest grid

spacing and this may cause wind direction artifacts in hurricane conditions.

The new ECMWF fifth Re-Analysis (ERA5) model data set is now available to the public and it replaces ERA-Interim [19]. With respect to the operational ECMWF model winds, ERA5 has been processed with one of the latest versions of the ECMWF Integrated Forecast System (IFS), albeit at lower grid spacing. Unlike ERA-Interim, ERA5 provides hourly forecasts for the whole time period of interest [20]. Under hurricane conditions, hourly forecasts are more suitable than 3-hourly forecasts since they provide a more precise location of the storm eyewall and center, at the scatterometer overpass time. Therefore, in order to have a consistently reprocessed data set favorable in hurricane conditions, we have reprocessed the OSI SAF/KNMI ASCAT-A wind data from 2009 to 2018 by using the ASCAT Wind Data Processor (AWDP) version 3.2 [21] with the new CMOD-7 GMF [5, 22] and the ERA5 10-m equivalent neutral winds, U_{10N} , in full resolution as background winds.

The hourly ERA5 U_{10N} winds have been downloaded through the ECMWF Meteorological Archival and Retrieval System (MARS) (<https://www.ecmwf.int/en/forecasts/datasets/archive-datasets>). They are used in the processing chain to perform ambiguity removal and quality control [21]. The former is carried out using a two-dimensional variational (2DVAR) ambiguity removal scheme [23]. The collocation between ASCAT and ERA5 wind is directly performed by AWDP. Three subsequent ERA5 forecast fields around the ASCAT acquisition time are used by AWDP to perform the interpolation, two forecast fields corresponding to UTC times before the ASCAT observing time and one after. Each of the three selected ERA5 forecasts is spatially interpolated to each ASCAT Wind Vector Cell (WVC) position. Then, a time interpolation of the three forecasts to the ASCAT acquisition time is performed to get the final collocated ERA5 wind vector components [24].

As shown in [6], the scatterometers measure the surface roughness which is more correlated with surface stress rather than with the 10 m surface wind speed. The surface stress is proportional to the air density and to the square of the equivalent neutral 10 m wind. In order to make the model winds more comparable to the scatterometer winds, a stress-equivalent correction should be applied. However, we have not converted the ERA5 U_{10N} to U_{10S} [3] at this stage, due to the downloading time of the ERA5 parameter GRIB files needed to carry out the conversion. This causes a systematic overestimation of the ERA5 wind by about 10% at 920 mb mean sea level pressure and which error is about linear with 0% error at 1013 mb. However, in terms of the wind data reprocessing, using model U_{10N} rather than U_{10S} , does not compromise the quality of the ASCAT wind speed retrievals.

C. Buoy Data

The buoys used in this study include the National Data Buoy Center (NDBC) moored buoys off the coasts of USA, the Ocean Data Acquisition System (ODAS) buoys in the north-east Atlantic and British Isles inshore waters, the NOAA Tropical Ocean Atmosphere (TAO) buoy arrays in the tropical Pacific, the Japan Agency for Marine-Earth Science and Technology

(JAMSTEC) Triangle Trans-Ocean Buoy Network (TRITON) buoys in the western Pacific, the Prediction and Research Moored Array in the Atlantic (PIRATA), and the Research Moored Array for African–Asian–Australian Monsoon Analysis and Prediction (RAMA) at the tropical Indian Ocean.

Two different types of buoy data sets are freely available to the users. The first data set consists of buoy winds that hourly report an averaged wind over 10 minutes, distributed through the Global Telecommunication System (GTS) stream, and quality controlled and archived through ECMWF MARS system (hereafter MARS buoy winds). Note that the MARS buoy winds are binned every 1 m/s in speed and 10 degrees in direction. The second data set consists of continuous 10-minute buoy wind measurements, further referred to as continuous buoy winds (hereafter Cwinds buoys). This data set is obtained from <http://www.pmel.noaa.gov/>, but it does not contain ODAS and TRITON continuous buoy winds.

In both buoy data sets, the measured wind vectors at a given anemometer height are converted to U_{10N} by using the Liu-Katsaros-Businger (LKB) model [25], in order to make them more comparable to ASCAT and ERA5 winds.

D. Best Track Data

The tropical cyclone “best track” (hereafter BT) data obtained from the WMO International Best Track Archive for Climate Stewardship (IBTrACS) [26] are used in this study in order to locate the storm center as sampled by each ASCAT overpass. In particular, we used the BT data set version v03r10, available at the NOAA National Climate Data Center (<https://www.ncdc.noaa.gov/ibtracs/>). However, at the time of this work, we noticed that in this data set there were few storms which did not have a complete BT record, i.e., for the whole duration of the storm. For those cases, the corresponding BT data available at the NOAA Hurricane Center have been used (<ftp://ftp.nhc.noaa.gov/atcf>). The BT data sets provide an estimate of the storm position every six hours for the whole duration of the storm. We carried out a linear interpolation in order to have a BT storm position every second (hereafter BTsec position) in line with the SFMR temporal sampling rate. The wind community still argues about the accuracy of the BT center estimates, notably when interpolated in between 6-hour periods. But, so far, the BT data set is the only source publicly available online, providing the storm positions for most of the storm duration.

III. METHODOLOGY

As already mentioned, we use ASCAT to compare buoy and SFMR wind estimates since the latter do not well collocate. Since the three data sources have different spatio-temporal characteristics (namely, sampling and resolution), different collocation approaches are implemented for ASCAT/SFMR and ASCAT/buoy comparisons.

A. ASCAT/SFMR collocation

The reprocessed ASCAT winds are collocated with SFMR winds by using SFMR storm-motion centric coordinates to allow collocations even when they are separated by a few hours

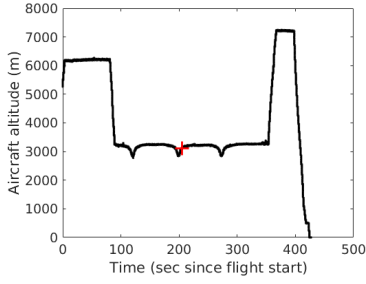


Fig. 1. NOAA flight SFMR170903H1 during Hurricane Irma on September 3rd, 2017. Aircraft altitude with respect to time, along with the altitude at t_{mean}^{SFMR} (red cross), the portion of the flight around 3 km corresponds to the aircraft storm-crossing operation.

in time. The underlying assumption is that within a certain temporal window (e.g., 2 or 3 hours), the hurricane structure does not change with respect to the direction of the storm displacement. As such, SFMR spatially and temporally varying observations are projected into a “frozen” hurricane structure during such temporal window. This is done by converting the SFMR coordinates into a new coordinate system identified by the BT position at the time of each SFMR sample.

Different options can be considered for the new coordinate system reference (i.e., the storm motion direction). One option is to use the motion vector derived from consecutive BTsec points at every SFMR (1-sec) sampled location. Note that best track data are six hours apart, meaning that all SFMR acquisitions within such time frame share the same storm motion vector. Although such option seems quite consistent since the conversion closely follows the storm track as seen by the BT data, it may cause artefacts when the SFMR flight occurs over two consecutive BT 6-hour periods and there is a change of the storm motion direction. Alternatively, one can use splines to smoothly interpolate over the BT 6-hour positions. However, the exact storm motion turn within the 6-hour period is unknown, which means that any interpolation strategy would lead to storm motion vector errors.

A more practical approach to avoid such artefacts is to use a single vector, which best represents the storm motion at the time of the SFMR flight or the ASCAT overpass. In this analysis, the BTsec position at the time corresponding to the middle of the temporal window over which the aircraft crosses the storm (t_{mean}^{SFMR}), is used to compute the single storm motion vector. The t_{mean}^{SFMR} value has been computed by using the mean time of the SFMR wind speed measurements within the highest 15% wind speed data. To validate this time value, the aircraft altitude has been used. In particular, during the storm crossings operation, the aircraft altitude is relatively constant, so that t_{mean}^{SFMR} can be seen as the time in the middle of the temporal window in which the aircraft stays at such operational altitude. An example of the typical aircraft altitude and the corresponding t_{mean}^{SFMR} is shown in Fig. 1. Once the best track position at t_{mean}^{SFMR} has been identified, the corresponding storm motion vector is selected as reference vector and used to convert the SFMR trajectory such that each SFMR point is referenced to the storm centre in polar coordinates. Figure 2a and 2b show an example of the trajectory of the NOAA flight H1 during Hurricane Irma on September

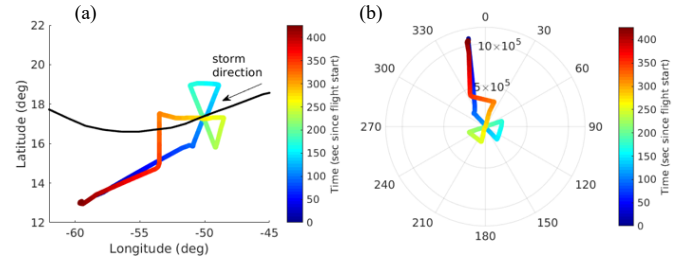


Fig. 2. NOAA flight SFMR170903H1 during Hurricane Irma on September 3rd, 2017. (a) Aircraft trajectory in original coordinates with respect to time (see colorbar), along with the BT data (black line); (b) Corresponding flight in storm-motion relative coordinates.

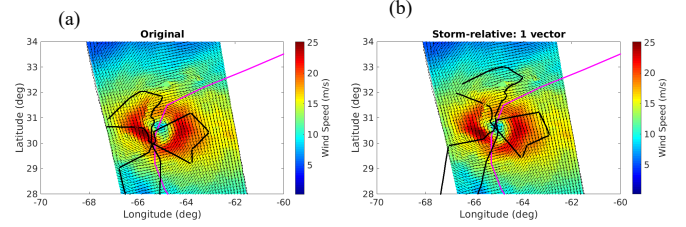


Fig. 3. ASCAT wind field over Hurricane Karl on September 23rd, 2016 along with the storm BTsec positions within a few hours from the ASCAT pass (magenta line). The black line corresponds to the NOAA I2 SFMR flight trajectory in original coordinates (a), and the storm-motion relative coordinates derived using a single vector (b).

3rd, 2017, in its original coordinates and in polar storm-motion relative coordinates, respectively.

It is important to mention that, due to the large variety of storm cases, the selected t_{mean}^{SFMR} may sometimes correspond either to the beginning or to the end of the storm crossing time window, depending on how strong the winds are within each cross. In the few cases in which the SFMR storm centre crossings are within two different BT 6-hour windows, different t_{mean}^{SFMR} estimation approaches may lead to either one storm motion vector or another. However, the use of one vector with respect to another, if close in time, does not significantly affect the results, since both are equally (un)certain. The main limitation of this methodology is that, besides the uncertainty in the BT data itself, the storm track is unknown within the six hours separating two best track points. As a consequence, the selected reference vector may not accurately describe the actual storm movement, especially if the storm rapidly changes during this time. We assume that the storm velocity is constant over the 6-hour period, which can be a rather crude assumption.

The converted SFMR trajectory is then relocated and centered on the BTsec position at the time of the ASCAT pass (t_{SCAT}^C). The ASCAT storm center and the corresponding BTsec point are selected as the ASCAT WVC/BTsec pair having time difference less than 1 sec and spatial distance less than $6.25\sqrt{2}$ km. When the ASCAT pass does not catch the whole storm structure and, in turn, the BTsec point is out of the ASCAT swath, the selected WVC is the one having spatial distance less than 200 km. The SFMR storm-motion centric polar coordinates are then converted into latitudes/longitudes by using the reference motion vector corresponding to the BTsec at t_{SCAT}^C . Figure 3a shows the ASCAT wind field over Hurricane

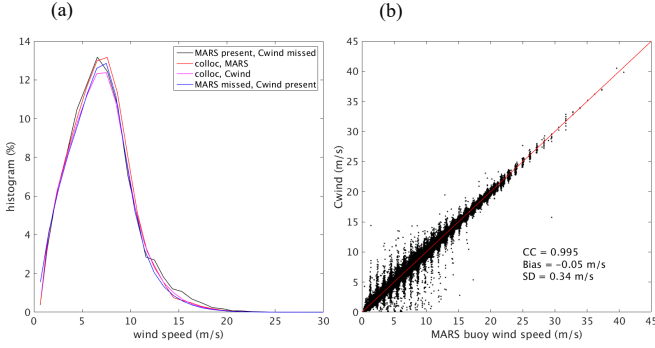


Fig. 4. (a) Histograms of the different buoy wind speed data sets. The black (blue) curve corresponds to the available MARS (Cwinds) buoy winds when the Cwinds (MARS) are missing; the red and magenta curves correspond to the collocated MARS winds and Cwinds, respectively, when both wind data sources are available. (b) Scatter plot of Cwinds speed versus MARS buoy wind speed. The scores of the correlation coefficient (CC), the bias, and the SD of the speed differences are shown in the legend.

Karl on September 23rd, 2016 along with the storm BTsec positions within a few hours from the ASCAT pass (purple line). The black line in Fig. 3a and Fig. 3b corresponds to the NOAA I2 SFMR flight trajectory in original and storm-motion relative coordinates, respectively.

Note that, the assumption on the “frozen” hurricane structure cannot hold for long time differences. Therefore, the time separation Δt between each SFMR wind acquisition and the ASCAT pass, as defined in (1), is taken into account to carry out the wind comparison:

$$\Delta t = |t_{SCAT}^C - t_i^{SFMR}| \quad (1)$$

where t_i^{SFMR} is the time of the collocated SFMR measurements. We have assessed the Δt impact on the wind comparison by carrying out an ASCAT/SFMR wind difference analysis at different Δt values, as explained in Section IV. B

B. ASCAT/MARS Buoy Collocation

To assess the consistency between MARS and Cwind buoys winds, we have first carried out a statistical analysis between these two data sets. To this end, five years of Cwinds and MARS buoy winds have been collocated from 2009 to 2014. The wind speed histograms are shown in Fig. 4a for different categories, such as: the distribution of the available MARS wind speed when the Cwind data are missing (black line) and vice versa (blue line); the distribution of the collocated Cwinds (purple line) and collocated MARS (red line) winds. The numbers of available collocations for each category are 3.4 million (black), 2.5 million (red), 2.5 million (magenta) and 4.4 million (blue), respectively. As shown by the red and the purple lines, the collocated MARS and Cwinds winds are consistent as they have very similar distributions, particularly for winds above 10 m/s. On the other hand, from the difference between the black and the blue curves above 10 m/s, it is clearly discernible that the MARS buoy data set has more high winds than the Cwinds. This is probably due to the fact that the MARS data set has more buoys at high latitudes (e.g., ODAS). When focusing on the high wind range, as shown in Fig. 4b, Cwinds and MARS buoy data sets are in good agreement, particularly

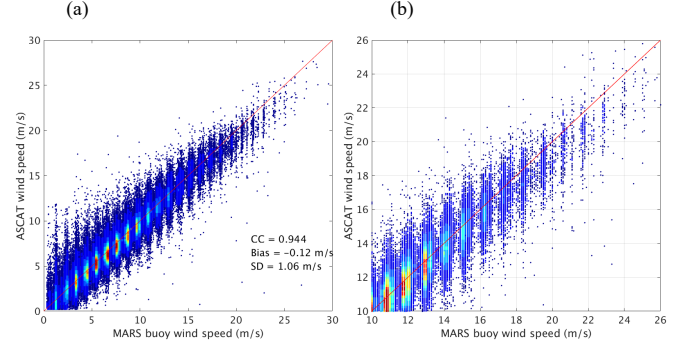


Fig. 5. (a) Scatter-density plot of ASCAT U_{10S} wind speed versus MARS buoy U_{10N} wind speed. The scores of the correlation coefficient (CC), the bias, and the SD of the speed differences are shown in the legend. (b) Same as shown in (a) but for wind speeds higher than 10 m/s.

for winds higher than 15 m/s. Therefore, the MARS buoy winds data set is favorable for high wind calibration, since it has more data in the high wind regime and it is seemingly of equal quality to that of the Cwinds buoy data. For this reason, the MARS data set is used in this study rather than Cwinds.

In order to collocate the MARS buoy winds with the ASCAT WVC winds, a temporal distance of 30 minutes along with a spatial distance of 25 km have been used. In case more than one WVC meets the collocation criteria, the closest WVC to the buoy acquisition has been used. A total amount of 350,000 collocations has been collected. The comparison between ASCAT and MARS buoys winds has been carried out in the whole wind speed range as well as by focusing only on the high wind regime. In the latter case, the winds speeds that meet the condition described in (2) are used:

$$15 \text{ ms}^{-1} < \frac{w_{ASCAT} + w_{buoy}}{2} < 25 \text{ ms}^{-1} \quad (2)$$

where w_{ASCAT} and w_{buoy} are the ASCAT U_{10S} and the buoy U_{10N} , respectively. A total of 9,700 collocations are collected in the high wind regime.

IV. RESULTS

A. ASCAT/Buoy Wind Comparison

The scatter-density plot of ASCAT wind speed versus MARS buoy wind speed is illustrated in Fig. 5a and Fig. 5b for the whole wind speed distribution and high winds, respectively. In general, there is very good agreement between ASCAT and MARS wind speeds, with a very high correlation coefficient (CC) of 0.94, a mean bias of -0.12 m/s and a standard deviation (SD) of 1.06 m/s. This is an expected result since buoy winds are used for ASCAT calibration purposes. When focusing only on high winds as described in (2), a higher bias of -0.30 m/s ($\sim 1.5\%$) is shown, while the standard deviation is only slightly larger (1.27 m/s), as compared to the overall distribution. This indicates that, on the one hand, there is a good agreement (low SD) between ASCAT and buoy high winds, and on the other hand, ASCAT U_{10S} winds slightly underestimate high winds

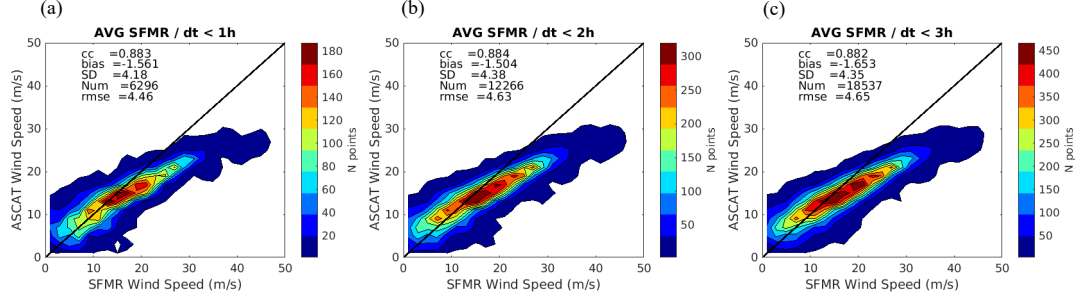


Fig. 6. Two-dimensional histograms of ASCAT and collocated SFMR wind speeds averaged over a distance of 12.5 km along track, for $\Delta t \leq 1h$ (a), $\Delta t \leq 2h$ (b), $\Delta t \leq 3h$ (c). The statistical parameters can be found in the legend, such as: correlation coefficient (cc), bias, standard deviation (SD), number of points (Num), root mean square error (rmse).

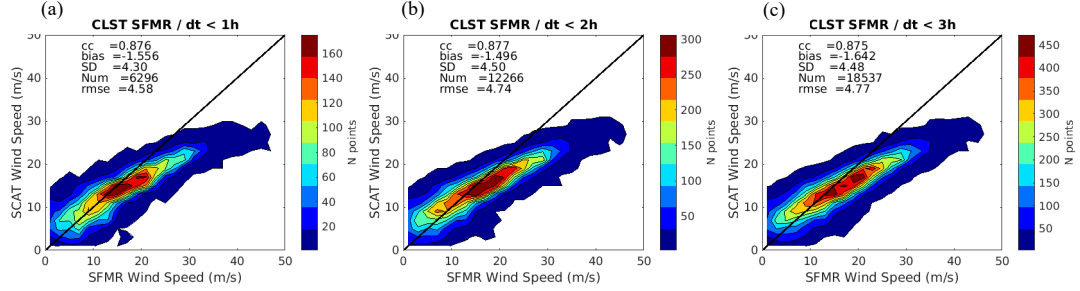


Fig. 7 Same as Fig.6, but for collocated spatially-closest SFMR winds within a maximum radius of $6.25\sqrt{2}$ km.

Table 1. Triple collocation standard deviation errors for u component (ε_u) and the v component (ε_v), at scatterometer scale, assuming that the r^2 value is $0.48 \text{ m}^2\text{s}^{-2}$ for both u and v components.

	MARS	ASCAT	ERA5
$\varepsilon_u \text{ (ms}^{-1}\text{)}$	1.13	0.57	1.33
$\varepsilon_v \text{ (ms}^{-1}\text{)}$	1.16	0.68	1.37

Table 2. Same as Table 1 but for high wind regime, i.e., using (2). The r^2 value is $0.63 \text{ m}^2\text{s}^{-2}$ and $1.00 \text{ m}^2\text{s}^{-2}$ for u and v components respectively.

	MARS	ASCAT	ERA5
$\varepsilon_u \text{ (ms}^{-1}\text{)}$	1.90	0.60	1.60
$\varepsilon_v \text{ (ms}^{-1}\text{)}$	2.08	0.69	1.52

with respect to buoy U_{10N} winds, in line with expectation [3].

In order to assess the quality of buoy winds above 15 m/s, we carried out a triple collocation (hereafter TC) analysis [27], which allows to estimate the errors and the calibration coefficients of three sets of collocated measurements. For this analysis the buoys (w_1), ASCAT (w_2), and ERA5 (w_3) winds have been used. As discussed in [28], to successfully calculate the individual random errors of each of the three collocated data sets, the representativeness error (r^2) needs to be accurately estimated. Such error represents the common short-scale true variance resolved by scatterometer and buoy winds, but unresolved by model winds. Here, the slope approach in [29] is used to estimate the r^2 value. That is, the r^2 value that leads to well intercalibrated data sets, such that the regression slopes of w_3 versus w_2 , and w_3 versus w_1 are both close to one. By using such method, the estimated r^2 value is $0.48 \text{ m}^2\text{s}^{-2}$ for both zonal (u) and meridional (v) wind components. Such value is smaller than the value presented in [4], which is estimated by integrating the spectral difference between the scatterometer wind and the ECMWF model winds. In [4], r^2 is $0.63 \text{ m}^2\text{s}^{-2}$ and $1.00 \text{ m}^2\text{s}^{-2}$ for u and v components, respectively. We have

analyzed the impact of varying r^2 values on the error standard deviations of the three data sets at the scale resolved by the scatterometer and the results reveal that both ε_u and ε_v are nearly independent on the r^2 . The ε_u and ε_v values for buoy, ASCAT, and ERA5 considering $r^2 = 0.48 \text{ m}^2\text{s}^{-2}$ and the whole wind speed range, are shown in Table 1.

To compute the TC standard deviation errors at high wind regime we have assumed the r^2 values equal to $0.63 \text{ m}^2\text{s}^{-2}$ and $1.00 \text{ m}^2\text{s}^{-2}$ for u and v components, respectively. Note that the wind variability (not shown here) does not show any remarkable changes at high wind conditions, therefore the r^2 value of the high winds is considered to be similar to that of the overall data set. Table 2 shows the results for high winds. With respect to Table 1, the error standard deviations for both MARS and ERA5 increases, indicating that there is a slight wind quality degradation at high wind regime, whereas ASCAT does not significantly vary. However, Fig. 5 clearly shows fairly good agreement between ASCAT and buoy, indicating that buoy winds can be used for calibration/verification purposes at high winds, up to 25 m/s [30].

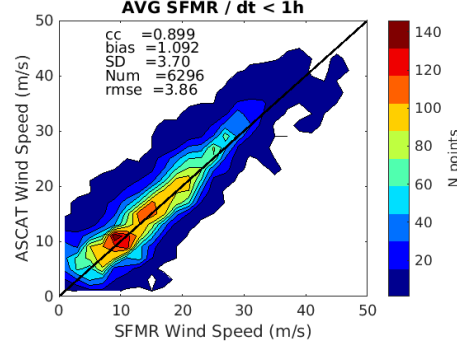


Fig. 8. Two-dimensional histograms of corrected ASCAT high winds and collocated SFMR wind speeds averaged over a distance of 12.5 km along track, for $\Delta t \leq 1$ h.

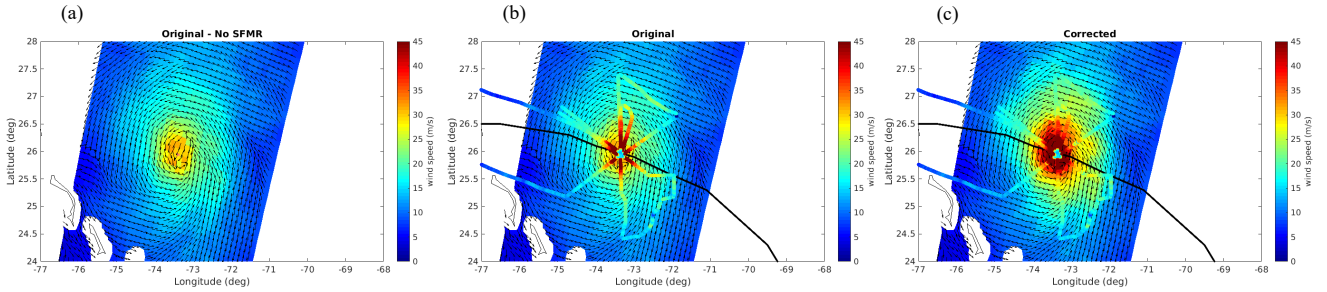


Fig. 9. ASCAT wind field over Hurricane Dorian on August 31st, 2019, along with the SFMR winds over the corresponding NOAA SFMR190831H1 flight trajectory. The black line shows the Hurricane Dorian BT positions. (a) ASCAT original wind field, (b) ASCAT original wind field with SFMR winds, (c) same as Fig. 9b but with the ASCAT corrected wind field.

B. ASCAT/SFMR Wind Comparisons

Two different strategies have been used to pair ASCAT winds with the storm-motion centric SFMR winds. The first comparison has been carried out by collocating ASCAT winds with spatially-averaged SFMR winds, i.e., averaged over a distance of 12.5 km along track. While this is not the same as the scatterometer measurement due to the shape of the averaging kernel [31], it makes the spatial scales more comparable. Figure 6 shows the two-dimensional histograms of the collocated winds for different temporal distances: $\Delta t \leq 1$ h (Fig. 6a), $\Delta t \leq 2$ h (Fig. 6b), $\Delta t \leq 3$ h (Fig. 6c). The results show that ASCAT underestimates winds in high wind regime with respect to SFMR. However, the wind comparison shows a reasonable scatter, with a standard deviation between 4.18-4.38 m/s. In addition, ASCAT and SFMR are very well correlated, with a correlation coefficient of about 0.88. As expected, the scatter increases with increasing Δt .

A similar analysis has been also performed by pairing ASCAT winds with the spatially-closest SFMR winds within a maximum radius of $6.25\sqrt{2}$ km. As shown in Fig. 7, also in this case the wind statistics improve as the time difference decreases. However, with respect to Fig. 6, the statistics between ASCAT and SFMR winds slightly worsen in terms of correlation coefficient as well as standard deviation, which now ranges between 4.3-4.5 m/s. This suggests that the averaged SFMR winds are more representative of ASCAT wind scales than the SFMR single measurements, as expected.

A relevant result from both Fig. 6 and Fig. 7 is that the

correlation between ASCAT and SFMR winds is relatively high, so that a suitable ASCAT wind scaling (calibration) may lead to very consistent high wind retrievals.

C. ASCAT High Wind Correction

An important result that arises from this indirect SFMR and MARS buoy wind inter-comparison is that both data sets are very well correlated with ASCAT at winds above 15 m/s. However, they show a different high-wind speed scaling. Although this does not allow to draw specific conclusions, at this stage, about which data set should be used as reference for scatterometer high-wind calibration/validation purposes, it also shows that with an appropriate high-wind re-scaling, both data sets can be made consistent with ASCAT.

Following the operational extreme winds community, which uses the dropsonde-based wind scaling as reference, we use the averaged SFMR winds to compute a correction to the ASCAT winds. Such correction aligns the ASCAT winds with SFMR and hence with dropsonde speeds. The resulting corrected ASCAT winds are hereafter referred to as ASCAT dropsonde-scale winds (since dropsondes are used to calibrate SFMR, which in turn is used to calibrate ASCAT high winds). The correction, as described in (3), is applied to ASCAT wind speed higher than 12 m/s winds.

$$U_{10s}^* = 0.0095U_{10s}^2 + 1.52U_{10s} - 7.6 \quad (3)$$

The results of the comparison between the ASCAT dropsonde-scale winds and the averaged SFMR winds, for Δt lower than 1 h are shown in Fig. 8. A higher correlation coefficient (0.9) and a lower mean bias (1.09 m/s) along with a lower standard deviation (3.70 m/s) are obtained with respect to the results shown in Fig. 6a, for wind speeds up to 40 m/s.

Fig. 9 shows an example of the ASCAT winds before (Fig. 9b) and after (Fig. 9c) applying the high wind correction for the case of the Hurricane Dorian on August 31st, 2019. The SFMR winds of the corresponding flight SFMR190831H1 in storm-motion relative coordinates are shown for comparison. Such wind correction allows ASCAT to better resolve the hurricane-force winds even close to the storm eye wall. The ASCAT and SFMR wind speeds better agree after the ASCAT wind correction, as expected. However, the low wind pattern within the storm eye is not well resolved by ASCAT (Fig. 9a), as expected by the small eyewall radius relative to the ASCAT spatial resolution.

V. CONCLUSION

Assessing the high and extreme wind capabilities of space-borne scatterometers is one of the main goals within the ocean wind community. Having a consolidated in-situ wind reference is crucial for the calibration and validation of passive and active microwave satellite winds. This work focuses on the collection, collocation, and analysis of two different high and extreme-wind data sets over a period of 10 years (2009-2018): SFMR and MARS buoy winds. To this end, the ASCAT winds are used as a stable reference to overcome the lack of buoy and SFMR wind collocations. Therefore, on the one hand, ASCAT is compared with SFMR winds and, on the other hand, ASCAT is compared with MARS buoy winds. MARS buoys are chosen in this work over the continuous buoy Cwind data since the former have more data in the high wind regime and they show equal quality in wind comparisons.

The ASCAT winds have been reprocessed using the new CMOD-7 GMF and the collocated ERA5 model winds as background winds. To collocate ASCAT WVCs winds with MARS buoy winds a temporal distance of 30 minutes along with a spatial distance of 25 km have been used. The closest WVC to the buoy acquisition has been used when more than one WVC meets the collocation criteria. The results show that the ASCAT wind products are in good agreement with collocated buoy winds up to 25 m/s. Air mass density effects, not yet accounted for, may show a slight underestimation of ASCAT U_{10S} with respect to buoy U_{10N} for winds above 15 m/s. This result is in line with expectation, since buoys are used to calibrate the operational Level 2 OSI SAF ASCAT wind product. Although buoy wind data comparisons slightly degrade under high wind conditions, they are generally found to be of good quality between 15 and 25 m/s, indicating that buoy winds can be used for high-wind calibration and validation purposes.

Different results are obtained when comparing ASCAT with SFMR winds. In order to collocate ASCAT and SFMR winds, the BT data from the IBTrACS dataset version v03r10, available at the NOAA National Climate Data Center along

with the BT data from the National Hurricane Center have been used to estimate hurricane mean motion. The SFMR trajectory has been converted into storm-motion relative coordinates. This allows to collocate SFMR with ASCAT even when they are separated by a few hours in time. However, such approach cannot be used for large time differences. Several sources of collocation errors have been reported, namely the BT temporal sampling, geolocation inaccuracies and the temporal differences between the SFMR and ASCAT acquisitions. The ASCAT/SFMR wind comparisons reveal a substantial underestimation of the ASCAT winds at wind speeds higher than 15 m/s. Despite such disagreement, ASCAT is well correlated with SFMR winds at high winds, with a correlation coefficient of about 0.88. The wind statistics slightly change depending on the time difference between ASCAT and SFMR acquisitions, with larger standard deviation of the differences with increasing time difference. In addition, it is shown that SFMR measurements averaged along track are more representative of the ASCAT resolved wind scales.

By using ASCAT as a reference to bridge SFMR and buoy measurements, we can conclude that both in situ wind sources are well correlated with ASCAT. However, large discrepancies between SFMR and buoy winds are present in the high wind regime, e.g., at 25 m/s the difference is $\sim 20\%$. Therefore, at this stage, conclusions cannot be drawn on which high-wind reference is favourable for scatterometer wind calibration/validation at high and extreme wind conditions. Further investigations are needed to better understand the sources of such differences [6]. However, these results show that with a suitable re-scaling, the ASCAT high winds become consistent with the SFMR winds after averaging over ASCAT footprints. A high wind calibration of ASCAT winds using averaged SFMR winds as reference shows good agreement between ASCAT and SFMR winds up to 40 m/s. The so-called ASCAT dropsonde-scale winds are made available for the operational extreme wind community, which uses SFMR wind scaling (as calibrated by dropsondes) as reference for tropical cyclone characterization, satellite and model wind calibration, monitoring, and tracking.

VI. REFERENCES

- [1] M. Belmonte Rivas and A. Stoffelen, "Characterizing ERA-Interim and ERA5 surface wind biases using ASCAT", *Ocean Sci.*, no. 15, pp. 831-852, 2019.
- [2] A. Trindade, M. Portabella, A. Stoffelen, W. Lin and A. Verhoef, "ERASTAR: A High-Resolution Ocean Forcing Product", *IEEE Trans. Geosci. Remote Sens.*, vol. 58, no. 2, pp. 1337-1347, 2020.
- [3] J. de Kloe, A. Stoffelen and A. Verhoef, "Improved Use of Scatterometer Measurements by Using Stress-Equivalent Reference Winds", *IEEE J. of Selected Topics in Applied Earth Observations and Remote Sensing*, vol. 10, no. 5, pp. 2340-2347, 2017.
- [4] J. Vogelzang, A. Stoffelen, A. Verhoef and J. Figa-Saldana, "On the quality of high-resolution scatterometer winds", *J. of Geophysical Research*, vol. 116, no. C10033, 2011.
- [5] A. Stoffelen, J. Verspeek, J. Vogelzang and A. Verhoef, "The CMOD7 Geophysical Model Function for ASCAT and ERS Wind Retrievals", *IEEE J. of Selected Topics in Applied Earth Observations and Remote Sensing*, vol. 10, no. 5, pp. 2123-2134, 2017, doi:10.1109/JSTARS.2017.2681806.
- [6] A. Stoffelen, A. Mouche, F. Polverari, G.-J. van Zadelhoff, J. Sapp, M. Portabella, P. Chang, W. Lin and Z. Jelenak, "C-band High and Extreme-

- Force Speeds (CHEFS)", EUMETSAT report, 2020. [Online]. Available: <https://www.eumetsat.int/CHEFS>.
- [7] L. Pineau-Guillou, F. Ardhuin, M.-N. Bouin, J.-L. Redelsperger, Bertrand Chapron, J.-R. Bidlot, Y. Quilfen, "Strong winds in a coupled wave-atmosphere model during a North Atlantic storm event: evaluation against observations", *Quarterly Journal of the Royal Meteorological Society*, vol. 114, pp. 317-332, 2018.
 - [8] "Stepped Frequency Microwave Radiometer (SFMR)—ProSensing". [Online]. Available: <https://www.prosensing.com/crb-product/sfmr/>.
 - [9] E. Uhlhorn and P. Black, "Verification of Remotely Sensed Sea Surface Winds in Hurricanes," *J. of Atmospheric and Oceanic Technology*, vol. 20, pp. 99-116, 2003.
 - [10] J.W. Sapp, S.O. Alsweiss, Z. Jelenak, P.S. Chang, J. Carswell, "Stepped Frequency Microwave Radiometer Wind-Speed Retrieval Improvements", *Remote Sensing*, vol. 11, no. 214, 2019.
 - [11] J.L. Franklin, M.L. Black, K. Valde, "GPS Dropwindsonde Wind Profiles in Hurricanes and Their Operational Implications", *Weather Forecast*, vol. 18, p. 32-44, 2003.
 - [12] E. Uhlhorn, P. Black, J. Franklin, M. Goodberlet, J. Carswell and A. Goldstein, "Hurricane Surface Wind Measurements from an Operational Stepped Frequency Microwave Radiometer", *Mon. Weather Rev.*, vol. 135, p. 3070-3085, 2007.
 - [13] M. Belmonte Rivas, A. Stoffelen, J. Verspeek, A. Verhoef, X. Neyt and C. Anderson, "Cone Metrics: A New Tool for the Intercomparison of Scatterometer Records", *IEEE J. of Selected Topics in Applied Earth Observations and Remote Sensing*, vol. 10, no. 5, pp. 2195-2204, 2017, doi:10.1109/JSTARS.2017.2647842.
 - [14] A. Verhoef, J. Vogelzang, J. Verspeek and A. Stoffelen, "Long-Term Scatterometer Wind Climate Data Records", *IEEE J. of Selected Topics in Applied Earth Observations and Remote Sensing*, vol. 10, no. 5, pp. 2186-2194, 2017, doi: 10.1109/JSTARS.2016.2615873.
 - [15] B. Klotz and E. Uhlhorn, "Improved Stepped Frequency Microwave Radiometer Tropical Cyclone Surface Winds in Heavy Precipitation", *J. of Atmospheric and Oceanic Technology*, vol. 31, p. 2392-2408, 2014.
 - [16] L. Ricciardulli, and F. Wentz, "Remote Sensing Systems ASCAT C-2015 Daily OceanVector Winds on 0.25 deg grid, Version 02.1", Santa Rosa, CA, Remote Sensing Systems. [Online]. Available: www.remss.com/missions/ascat. Accessed on March 29, 2021.
 - [17] L. Ricciardulli, "ASCAT on MetOp-A Data Product Update Notes", Remote Sensing System Technical Report, [Online]. Available: www.remss.com/missions/ascat. Accessed on March 29, 2021.
 - [18] S. Soisuvarn, Z. Jelenak, P. S. Chang, S. O. Alsweiss, and Q. Zhu, "CMOD5.h—A high wind geophysical model function for C-band vertically polarized satellite scatterometer measurements", *IEEE Trans. Geosci. Remote Sens.*, vol 51, pp. 3744-3760. doi: [10.1109/TGRS.2012.2219871](https://doi.org/10.1109/TGRS.2012.2219871)
 - [19] "Copernicus Climate Change Service (C3S) (2017): ERA5: Fifth generation of ECMWF atmospheric reanalyses of the global climate . Copernicus Climate Change Service Climate Data Store (CDS). <https://cds.climate.copernicus.eu/cdsapp#!/home>".
 - [20] H. Hersbach and D. Dee, "ERA5 Reanalysis is in Production", *ECMWF Newsletter*, vol. 147, 2016.
 - [21] A. Verhoef, J. Vogelzang, J. Verspeek and A. Stoffelen, "AWDP Users Manual and Reference Guide, version 3.2", EUMETSAT NWP-SAF Report, 2018. [Online]. Available: https://www.nwpsaf.eu/site/download/documentation/scatterometer/AWDP/NWPSAF-KN-UD-005_AWDP_User_Guide_v3.2.pdf.
 - [22] A. Verhoef and A. Stoffelen, "ASCAT Wind Product User Manual version 1.16", EUMETSAT OSI-SAF Report, 2019. [Online]. Available: https://scatterometer.knmi.nl/publications/pdf/ASCAT_Product_Manual.pdf.
 - [23] J. Vogelzang, A. Stoffelen, A. Verhoef, A. Bonekamp, "Validation of two-dimensional variational ambiguity removal on SeaWinds scatterometer data", *J. of Atmospheric and Oceanic Technology*, vol. 26, pp. 1229-1245, 2009. doi: 10.1175/2008JTECHA1232.1.
 - [24] W. Lin, M. Portabella, A. Stoffelen, J. Vogelzang, A. Verhoef, "On Mesoscale Analysis and ASCAT Ambiguity Removal," *Quarterly J. of the Royal Meteorological Society*, vol. 142, no. 697, pp. 1745-1756, 2016.
 - [25] W. T. Liu, K. Katsaros, and J. Businger, "Bulk Parameterization of Air-Sea Exchanges of Heat and Water Vapor Including the Molecular Constraints at the Interface", *J. of Atmospheric Sciences*, vol. 36, pp. 1722-1735, 1979.
 - [26] K.R. Knapp, M.C. Kruk, D.H. Levinson, H. J. Diamond, and C. J. Neumann, "The International Best Track Archive for Climate Stewardship (IBTrACS): Unifying tropical cyclone best track data", *Bulletin of the American Meteorological Society*, vol. 91, pp. 363-376, 2010.
 - [27] A. Stoffelen, "Toward the true near-surface wind speed: Error modeling and calibration using triple collocation", *J. of Geophysical Research*, vol. 103, 1998.
 - [28] W. Lin, M. Portabella, A. Stoffelen, J. Vogelzang, and A. Verhoef, "ASCAT wind quality under high subcell wind variability conditions", *J. of Geophysical Research Oceans*, vol. 120, p. 5804-5819, 2015.
 - [29] N. Hoareau, M. Portabella, W. Lin, J. Ballabrera-Poy and A. Turiel, "Error Characterization of Sea Surface Salinity Products Using Triple Collocation Analysis", *IEEE Trans. Geosci. Remote Sens.*, vol. 56, no. 9, pp. 5160-5168, 2018.
 - [30] J. Edson, D. Vandemark, and M. Emond, "Evaluating several key issues in satellite wind stress validation", IOVST meeting, Barcelona Spain, April 24-26, 2018. [Online]. Available: mdc.coaps.fsu.edu/scatterometry/meeting/docs/2018/docs/WednesdayApril25/WednesdayMorning_vandemark_edson_OVW2018_talk.pptx.
 - [31] J. Vogelzang and A. Stoffelen, "ASCAT Ultrahigh-Resolution Wind Products on Optimized Grids", *IEEE J. of Selected Topics in Applied Earth Observations and Remote Sensing*, vol. 10, no. 5, pp. 2332-2339, 2017, doi: 10.1109/JSTARS.2016.2623861.



Federica Polverari received the M.Sc. degree in electronic engineering from Sapienza University of Rome, Rome, Italy, in 2013, and the Ph.D. degree in the Information and Communication Technologies-Radar and Remote Sensing, in 2017.

From 2017 to 2019 she was a Postdoctoral Researcher in radar scatterometry, at the Institut de Ciències del Mar, Barcelona, Spain. In 2019 she was awarded a NASA Postdoctoral Program Research Fellowship at NASA Jet Propulsion Laboratory, California Institute of Technology, Pasadena, CA,

USA. Her research interests include active microwave remote sensing of ocean surface winds with focus on the characterization of extreme wind retrieval capabilities of spaceborne scatterometry using airborne radiometry and in-situ wind measurements, scatterometer geophysical model function development, modeling and characterization of the ocean surface scatterometer response.



Marcos Portabella was born in Barcelona, Spain, in 1970. He received the B.Sc. degree in physics from the University of Barcelona, Barcelona, Spain, in 1994, the M.Sc. degree in remote sensing from the Institute of Space Studies of Catalonia, Barcelona, in 1995, and the Ph.D. degree in physics from the University of Barcelona.

He is currently with the Institut de Ciències del Mar, Barcelona, Spain, where he is involved in satellite remote sensing, and particularly scatterometry and L-band radiometry



Wenming Lin (Senior Member, IEEE) was born in Fujian, China, in 1984. He received the B.Sc. degree in engineering from Wuhan University, Wuhan, China, in 2006, and the Ph.D. degree in engineering from the National Space Science Center, Chinese Academy of Sciences, Beijing, China, in 2011. From 2011 to 2017, he was a Postdoctoral Researcher with the Institut de Ciències del Mar, Barcelona, Spain, focusing on the advanced oceanographic data processing methods, remote sensing of ocean surface winds, and data assimilation. He is currently a Faculty Member with the Nanjing University of Information Science and Technology (NUIST), Nanjing, China, focusing on ocean remote sensing.



Joseph W. Sapp (Member, IEEE) received the B.S. degree in electrical engineering from The Pennsylvania State University, University Park, PA, USA in 2006, and the Ph.D. degree in electrical and computer engineering from the University of Massachusetts Amherst, Amherst, MA, USA, in 2015.

From 2006 to 2009, he was a Project Electrical Engineer with Lutron Electronics Company, Inc., Coopersburg, PA, USA, during which he was involved in the embedded software design of multiple commercial products. In 2009, he joined the

Microwave Remote Sensing Laboratory, University of Massachusetts Amherst, to complete his graduate work. During this time, he had the opportunity to begin participating in flights with the National Oceanic and Atmospheric Administration (NOAA) Hurricane Hunters. Since 2015, he has been with NOAA/National Environmental Satellite, Data, and Information Service (NESDIS)/Center for Satellite Applications and Research (STAR), College Park, MD, USA, as a Support Scientist with Global Science and Technology, Inc., Greenbelt, MD, USA. His recent research involves using active, passive, and in situ sensors together to improve the algorithms and equipment used in remote sensing of ocean surface and atmospheric wind vectors in extreme environments.



Paul S. Chang (Senior Member, IEEE) received the B.S. degree in electrical engineering from the Union College, Schenectady, NY, USA, in 1988, and the Ph.D. degree in electrical engineering from the University of Massachusetts Amherst, Amherst, MA, USA, in 1994.

Since 1994, he has been a Research Physical Scientist with the Center for Satellite Applications and Research, National Environmental Satellite, Data and Information Service (NESDIS), National Oceanic and Atmospheric Administration (NOAA). Current

activities include research and development in active and passive microwave remote sensing of the ocean surface with an emphasis on retrieval of the ocean surface wind field. Wind retrieval algorithm improvements and new product developments are pursued through the analyses of satellite and aircraft microwave remote sensing data. An emphasis is placed on transitioning research results into operational use, which involves cooperative relationships with the operational facets of NESDIS and with the National Weather Service, a primary end user of these data. Current efforts are focused on working on the METOP-ASCAT, SCATSAT, CFOSAT, CYGNSS, and GCOM-W missions in addition to planning and risk reduction activities for future ocean vector winds missions.



Ad Stoffelen (Senior Member, IEEE) received the M.Sc. degree in physics from the Technical University of Eindhoven, Eindhoven, The Netherlands, in 1987, and the Ph.D. degree in meteorology on scatterometry from the University of Utrecht, Utrecht, The Netherlands, in 1998. He currently leads a Group on active satellite sensing with the Royal Netherlands Meteorological Institute, De Bilt, The Netherlands, where he is involved in the future missions and research and development of retrieval to 24/7 operations, numerical weather prediction (NWP)

mesoscale wind data assimilation, user training, and services. He is also with the European Space Agency Doppler Wind Lidar Mission—Aeolus—on atmospheric dynamics. His research interests include establishing an international scatterometer virtual constellation.



Zorana Jelenak (Member, IEEE) received the Ph.D. degree in physics from the Waikato University, Hamilton, New Zealand, in 2000.

In March 2001, she joined the Ocean Winds Team, National Oceanic and Atmospheric Administration (NOAA)/National Environmental Satellite, Data, and Information Service (NESDIS)/Office of Research Applications (ORA), as a University Corporation for Atmospheric Research (UCAR) Visiting Scientist. She is a member of the NASA Ocean Surface Winds Science Team, a NOAA's Environmental Data Record

(EDR) Algorithm Lead for the AMSR-2 radiometer, and a member of the NASA CYGNSS Science Team. Her interests are in ocean surface wind vector measurements from active and passive microwave measurements and its applicability in an operational near-real time environment, retrieval algorithm development, model function development, advanced statistical analysis, and error analysis for improved algorithm characterization.